Feasibility of EIS on Module Level Li-ion Batteries for Echelon Utilization

A. Savca[1], S. Azizighalehsari[1,*], P. Venugopal[1], G. Rietveld[1,2] and T. Batista Soeiro[1]
[1]Power Electronics & EMC Group, University of Twente, Enschede, The Netherlands
[2]VSL, Delft, The Netherlands
* E-mail : s.azizighalehsari@utwente.nl

Abstract—The exponential growth in electric vehicles causes similar growth in retired batteries, resulting in a need to evaluate these batteries for possible use in other applications. Methods for fast health characterization are still challenging for batteries. So far, electrochemical impedance spectroscopy as a frequency domain measurement technique has been mainly used for this purpose at the battery cell level. This paper aims to evaluate the feasibility of EIS on the module level, to see whether it allows obtaining the module's practical electrical equivalent circuit model (ECM) beyond cell-level modeling. To this end, ECM parameters derived from EIS measurements on cells are compared with those from modules made from these cells. The results show a clear correlation between measuring the EIS on the cell level and the module created by connecting the same cells. This provides a first evidence for the usefulness of conducting EIS measurements at module level with an acceptable range of accuracy and consistency with the results obtained from the individual cells.

Keywords— Lithium-ion Battery (LIB), Equivalent Circuit Model (ECM), Electrochemical Impedance Spectroscopy (EIS), Second Life Batteries (SLB), Battery Module.

I. Introduction

The European Union (EU) has set a pioneering goal to significantly reduce greenhouse gas emissions to at least 55% compared to recorded emissions from 1990. It is one of the main objectives of the EU 2030 Climate Target Plan [1]. The transportation system has always had a significant share in pollution by relying on burning fossil fuels. Electrification of the transportation systems in both public and private sectors has been considered a major solution to mitigate the ramification of climate change and global warming. Fortunately, the growth of electric vehicles (EVs) is happening drastically worldwide, especially in the EU. Batteries, particularly Li-ion batteries, play a leading role in enabling vehicles to run independently from fossil fuels [2]. Fig. 1 shows the rapid growth of the battery electric vehicle stock from 2011 to 2020 with a comparison between Europe and the rest of the world. Besides the worldwide expansion of batteries, there are significant concerns about the maturity of this technology, including insight into the capacity degradation over time [3]. The battery state of health (SOH) is an indicator to define the level of capacity degradation. It is generally defined as the ratio of actual current capacity, and nominal capacity of the battery [4].

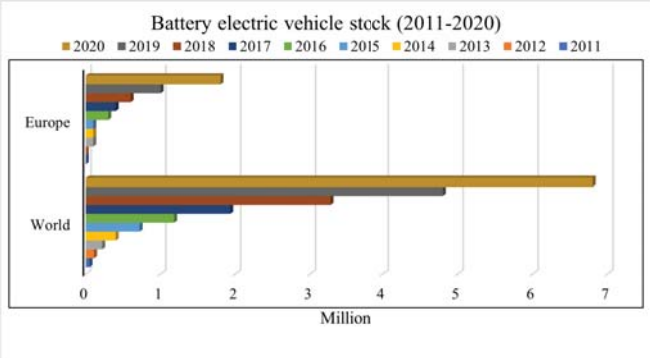

Fig. 1. Battery electric vehicle stock [5]. The increase in the stock of EVs is showing an exponential trend, with Europe alone accounting for approximately 20% of the global EV stock of 6.8 million EVs in 2020.

Car manufacturers typically set a limit of around 20-30% of reduction in SOH of batteries as the threshold for its application in EV [6]. This indicates the End of Life (EOL), meaning that the role of the battery in its first-life application is deemed complete, and the battery should be replaced and be evaluated for a possible second-life application. The number of projects that are running on second-life batteries is growing rapidly in Europe [7], [8]. To evaluate the usability of the battery for specific applications, it is necessary to evaluate the SOH of the battery before starting the re-purposing process. The key is to know the SOH of the modules inside the battery pack since the aging of the modules inside the pack is not uniform. Also, to reduce the failure rate of battery packs for second-life applications, combining modules with the same health condition into a new battery pack is critical [9].

By performing the capacity test, the battery's current capacity can be measured, and then the SOH can be calculated by comparing the measured value with the nominal capacity. Unfortunately, the capacity itself is not sufficient to give information about the degradation inside the battery. To achieve a better understanding of the actual battery health condition, it is essential to have knowledge of additional parameters that provide information on their internal features, like the impedance of the battery.

A comprehensive analysis of different SOH assessment methods for retired batteries has been done in [10], e.g., incremental capacity analysis (ICA), differential voltage analysis (DVA), differential thermal voltammetry (DTA), electrochemical impedance spectroscopy (EIS), etc. In [10], the analysis is performed at the cell level, while analysis in the module level is missing. It is interesting to perform analysis on a battery module because it facilitates and speeds up the characterization process. This paper is looking for a fast and accurate method for determining the battery cell internal parameters of an equivalent circuit model (ECM) which are related to its internal degradation. First, the measurement methodology for EIS at cell level and for a module consisting of the same cells connected in series is discussed. Subsequently, EIS measurements are performed on cells and module at different state of charge (SOC) levels, and from these measurements, the parameters of an ECM are determined. The relation between these parameters for single cells and for the module with the same cells connected in series is evaluated. Based on these findings, a conclusion is drawn on the applicability of EIS at module level.

II. Theoretical background

A. EIS as a method for SOH estimation

The SOH provides a rough estimate of how the battery ages and degrades over time, and it can serve as a signal for when the battery should be reused or repurposed. Essentially, the SOH measures how closely the current state of one or more parameters in a lithium-ion battery compares to the ideal state of those same parameters. Additionally, different battery uses may require different combinations of parameters to determine its SOH [8], [11].

Determining the SOH of Li-ion batteries poses several challenges, especially for their second life, which can be either internal or external. Internal challenges are related to battery chemistry and include the complex degradation process of Li-ion batteries, which occurs in 3 stages: loss of Li inventory, loss of active positive electrode material, and negative electrode material [12]. Each individual mode has distinct effects on battery health, which can be measured. Additionally, due to variations in raw materials and manufacturing processes, even batteries with the same chemical composition can have different structures and physical properties. External challenges are related to environmental factors, such as temperature and humidity, and can have varying effects on battery health. Furthermore, distinct driving regimes affect the battery SOH differently.

Compared to other methods for estimating the SOH, the EIS method has several advantages. Firstly, it is a fast method that gives information about the SOH of the battery. EIS can provide information on various internal parameters and processes within the battery. These include internal resistance, charge transfer resistance, solid electrolyte interface (SEI) layer, diffusion processes, and double-layer capacitance. This information can provide insight into ageing mechanisms inside the battery. Additionally, EIS is a harmless method that does not change or alter the battery's functioning. However, there are some disadvantages to using the EIS method. It is an offline method, which means the batteries must be in a steady state or disconnected. Additionally, EIS needs complex machinery such as potentiostats, voltage/current boosters, and frequency response analyzers (FRAs) [13].

Usually, the second-life modules provide no access to individual cells, so performing the EIS on modules is highly preferred. Nevertheless, the current research studies the EIS mostly on individual cells. Examples of EIS applied on modules are scarce, and only two examples could be found: [13], and [14]. Although these papers apply the EIS on module level, they do not investigate its reliability and whether the same methods can be applied to modules instead of cells.

B. EIS Theory

EIS is a commonly used method for electrochemical measurements that involves applying a small alternating current (AC) signal to an electrochemical cell and then measuring the resulting outcome. By looking at the impedance and phase difference between the input and the output at different frequencies, it is possible to distinguish between different electrochemical processes with different time constants. There are two main methods for performing EIS: potentiostatic EIS (PEIS), in which an AC voltage is used as an input and the AC current response is measured, and galvanostatic EIS (GEIS), where the AC current signal is applied to the battery and the voltage in response is measured [15].

To obtain accurate EIS measurements, certain conditions must be maintained. Causality requires that the response at any given time results from the input that occurred before that time and is not influenced by any subsequent signals. The linearity property is maintained by using a small AC signal, typically in the range of 5-25mV, and checking that the output voltage signal in GEIS is fitting in this range. Time-invariance is also important for obtaining valid EIS measurements [15].

To maintain time invariance in Li-ion batteries, a relaxation time is necessary for them to reach a steady state. External disturbances should be avoided to ensure that the output solely depends on the input.

PEIS is used to analyze systems with high-impedance to prevent high currents at the output, which can lead to poor SNR. GEIS is used for low-impedance systems because the commercial galvanostats are more accurate than the potentiostats for this situation.

The impedance spectrum obtained from the EIS is usually visualized in a Nyquist plot where the real part of the impedance is plotted against the imaginary part. This enables the analysis of the battery's electrochemical behavior in a wide frequency range. This plot helps to parameterize the capacitance, internal resistance, and inductance of the cell components [16].

C. The equivalent circuit model

One challenge of using the EIS technique is analyzing and interpreting the outcome obtained from the Nyquist plots. A

common approach to analyze EIS data is by circuit modeling. In this method the electrical circuits are linked to processes inside the battery. Even though it gives a lot of information about the battery's state it has the disadvantage of over-parametrizing and misinterpreting the results. Therefore it is vital to employ the elements that can be explained in terms of their physical characteristics linked to the battery internals or processes.

In order to apply the ECM technique, one can make use of fitting algorithms widely available. The process involves adjusting the simulated spectrum from the parameters to achieve a match with the measured spectrum. This fitting process aims to minimize the differences between the two spectra. This process does not need complex computation, which makes the battery management system (BMS) less complicated.

This method is powerful since with the parametrized ECM elements, one can quantify the battery states, e.g., SOC, SOH, and remaining useful life (RUL). The elements that are commonly used in ECMs include resistors (R), capacitors (C), inductors (I), Warburg elements (W), and constant phase elements (CPE or Q) [16]. Fig. 2 illustrates a model representing the entire Li-ion battery.

The model's complexity needs to be simplified to make impedance analysis practical. First of all, the separator capacitance (C_{SEP}) can be disregarded as it has a negligible value compared to the other capacitances. In addition, since the EIS spectra mostly come from the working electrode, the counter-electrode elements can be safely ignored. The series resistances R_{Cu}, R_{elec}, R_{Al} can also be combined into a single resistance. Consequently, the overall equivalent circuit for a half-cell Li-ion battery is obtained through simplification [17]. Fig. 3 shows the most commonly used ECM for Li-ion battery half-cells.

III. Method and Experimental Set-up

A. Methodology

The following approach is used to quantify the applicability of EIS measurement on module-level Li-ion batteries. First, one performs EIS for each individual cell. The cells in this study are Li-ion Panasonic NCR 18650 PF with nickel-manganese-cobalt (NMC) chemistry. Subsequently, up to six cells are connected in series one by one from one up to six cells to form a module. However, step by step after each added cell EIS is measured. The resulting EIS measurements are analyzed using a Nyquist plot and a second-order ECM, as shown in Fig. 4. From each EIS curve, the values of the different components in the second-order ECM model are obtained by data fitting. Furthermore, the ECM components for every single cell are summed and then compared to the ECM components of the whole module. The difference between these two results shows to what extent EIS performed on Li-ion modules gives a good indication of the properties of the individual cells in the module. This approach has been done for the module at different SOC to see the method's applicability at different SOC levels. The ECM shown in Fig. 4 is a typical half-cell system applied to batteries of NMC chemistry. The inductor L was used for achieving a better curve fit, however, its values are not used in the further analysis as they are strongly influenced by the equipment's inductance and therefore provide no meaningful information about the battery chemistry. The R_{SEI} and C_{SEI} reveal information about the state of the solid electrolyte interface (SEI) layer inside the battery. They can be linked to the first RC semi-arc in the EIS plot. Subsequently, R_{ct} and C_{dl} show the state of the double layer in the battery. They can be linked to the second RC semi-arc that has a higher radius than the first

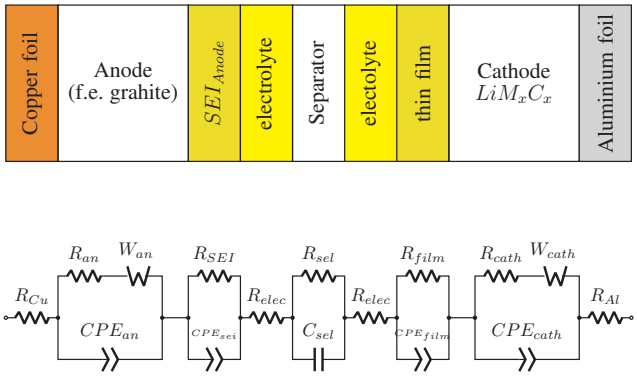

Fig. 2. Model representing the complete circuit of a lithium-ion battery. This model comprehensively explains the battery electrochemical processes in action and the physical elements linked with it [17].

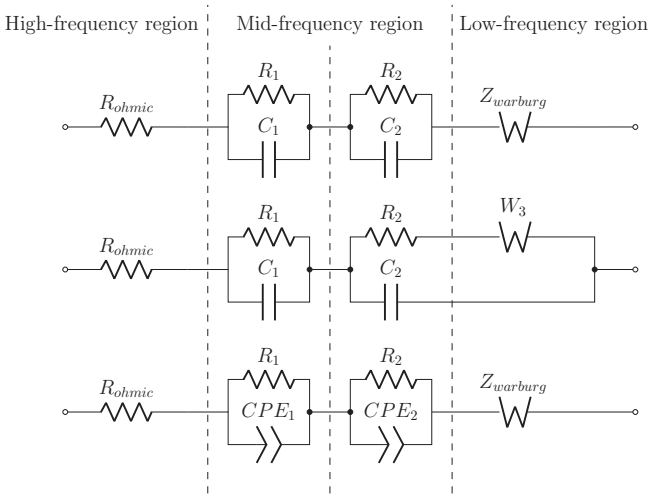

Fig. 3. Different equivalent circuit models used for Li-ion batteries, with the most suitable model depending on the chemistry of the battery [18].

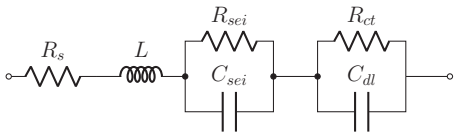

Fig. 4. Equivalent circuit model (ECM) used for analysing and interpreting the EIS measurements in this paper.

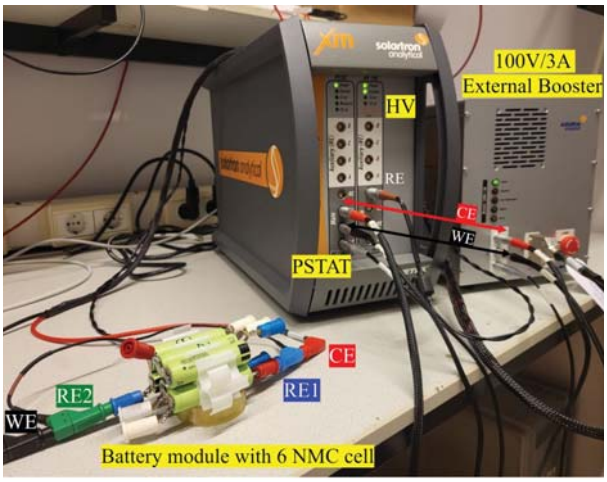

(a)

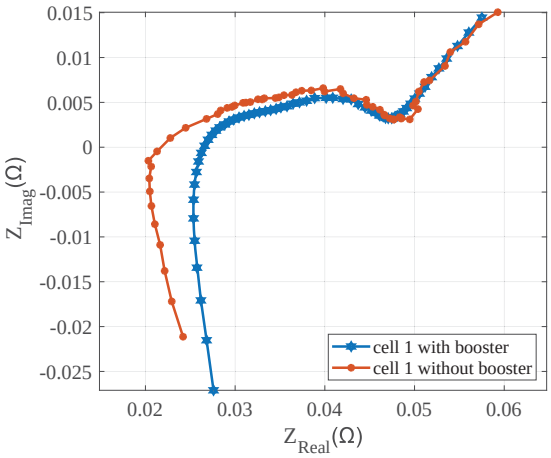

(b)

Fig. 5. Experimental EIS set-up including current booster (a), and the difference in EIS results on cell 1 with and without using the booster (700 mA and 100 mA current level respectively) (b). It is easy to observe that the small-signal EIS measurements without the booster is inaccurate especially for small values of impedance, necessitating an amplifier stage.

one since R_{ct} is the largest resistance component in the total resistance of a lithium-ion battery [19]. The Warburg element will not be used in the ECM as the diffusion processes are not of interest in this paper.

B. Measurement Equipment and EIS Test Settings

A Solarton EchemLab XM was used for the EIS measurements, equipped with a 100 V / 3 A booster. The EIS is performed in galvanostatic mode since this mode has more current ranges than the potentiostatic mode, indicating that the current through the cell can be controlled more accurately than the voltage. The booster has been used as shown in Fig. 5(a) to boost the amplitude of the injected current in high voltage (HV) range.

The current level was set such that a sufficient signal was achieved in the EIS module level measurements, whereas at the same time, the current should be low enough for the EIS measurements to be in the linear regime of the cell. Initially, the test results created by selecting 100 mA current led to a measurement of only 2.5 mV (25 mΩ cell impedance) which is insufficient for the HV mode accuracy according to the specifications of the EIS instrument. Therefore, one increased the injected current signal and measured the voltage signal in response to reach the accurate range of the device. Therefore, the final current amplitude was chosen as 700 mA, which resulted in a voltage signal of around 17.5 mV. This is still not in the optimal accuracy range of the HV mode of the EIS instrument, however, at this amplitude, the cells are still in the linear regime while the module measurements can still be measured with an accuracy of 1-3%.

In order to illustrate experimentally why the booster has to be used, an EIS test on one cell is performed with and without the booster at 700 mA and 100 mA current respectively. In Fig. 5(b) it can be seen that the EIS spectrum obtained without using the booster suffers from noise and thus is less reliable. The whole set-up with the booster is shown in Fig. 5(a). The frequency range in the measurements was chosen such as to cover all EIS regions (inductive, resistive, capacitive and diffusion region) and is from 10 kHz down to 10 mHz.

IV. Results & Discussion

The EIS of all six cells was measured according to the method explained in section II, and subsequently, the ECM parameters were obtained by fitting the data of each Nyquist plot. The results from the galvanostatic measurements at cell and module level when the cells are fully charged (100% SOC) are given in Fig. 6 and Fig. 7. The resulting ECM parameters at 100% SOC are given in Table I based on the data from Fig. 6 (cells) and Fig. 7 (module). For other SOCs, the same procedure was followed, and the final results, i.e., relative deviations between module results and sum of cell results, for 40% SOC and 10% SOC are given in the last two rows of Table I.

The data in Table I shows that the relative error between the combined single-cell EIS and the whole module EIS at 100% SOC for all the ECM parameters is less than 6.5%. This deviation can also be visualized graphically in Fig. 7.

The highest error was obtained for the series resistance R_s. This can be explained by Solartron equipments error that is directly proportional to the frequency of the signal. So for a higher test frequency the EIS plot will have a higher deviation meaning that the higher frequency parameters will do as well. On the other hand for the higher frequency parameters the errors decreases.

The errors are attributed to unwanted effects from the measurement set-up connections. For instance, there are stray capacitances resulting from the interconnections between the cells and additional resistances that are not present when mea-

TABLE I
THE ECM PARAMETERS OF SINGLE NMC CELLS AND WHOLE NMC MODULE AT 100% SOC (TOP PART). THE LAST TWO ROWS SHOW THE FINAL RESULT AT 40% AND 10% SOC.

Parameters / Tested	$R_s[m\Omega]$	$R_{SEI}[m\Omega]$	$C_{SEI}[F]$	$R_{ct}[m\Omega]$	$C_{dl}[F]$
Cell 1	25.60	11.55	0.234	73.02	5.08
Cell 2	24.40	11.93	0.235	77.91	5.06
Cell 3	24.66	13.50	0.204	102.97	4.80
Cell 4	25.76	13.28	0.197	98.47	4.76
Cell 5	26.36	14.07	0.161	85.93	4.59
Cell 6	24.98	14.19	0.184	98.86	4.75
Cell 1-6 in series	142.34	78.31	0.0323	524.13	0.801
Sum of all 6 cells	151.76	78.52	0.0332	537.16	0.805
Relative deviation at 100% SOC	6.2%	0.2%	2.7%	2.4%	0.5%
Relative deviation at 40% SOC	6.0%	5.4%	1.6%	4.6%	1.0%
Relative deviation at 10% SOC	4.3%	1.0%	1.8%	0.9%	1.3%

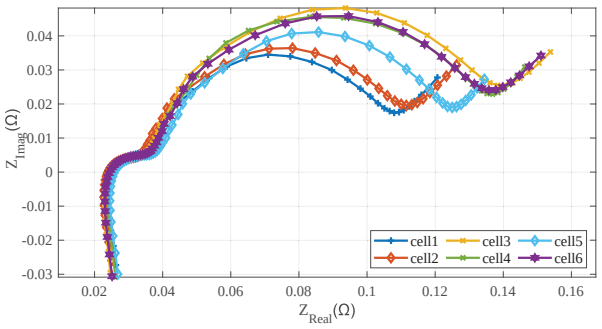

Fig. 6. Nyquist plots of the impedance characteristics of the six NMC cells studied in this paper, based on EIS measurement of each cell at 100% SOC. The frequency in the measurements ranges from 10 kHz down to 10 mHz. The difference in the second semi-arc radii is due to ageing effects on the charge transfer resistance, double layer capacitance, and the uncertainty in the SOC for each cell.

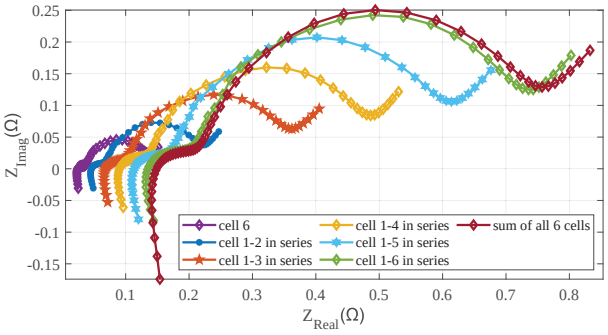

Fig. 7. Nyquist plot of the impedance characteristics of the modules made by connecting individual NMC cells in series based on EIS measurement at 100% SOC. The frequency in the measurements ranges from 10 kHz down to 10 mHz. The discrepancy between the module level measurement and the sum of individual cells is created due to parasitic inductance of the busbar, stray capacitance, and instrumentation inaccuracies. The maximum discrepancy observed is for the series resistance at 100% SOC.

suring only single cells. Moreover, the errors can be attributed to inaccuracies in the fitting algorithm used for modeling the cells and each module. To further evaluate this, more models can be used to check whether they give a better fit for the tested batteries. Finally, part of the errors can be attributed to inaccuracies in the electrochemical EIS workstation, as mentioned in section II. However, tests performed at different SOC levels give almost similar results with an error between 0-6.5%.

The results from Table I suggest that there is a correlation between the electrical parameters of individual cells and the parameters of the whole module. However, this does not mean that the SOH estimation methods using EIS can be applied to Lithium-ion modules in the same manner as to individual cells. This can be explained through the situation where 2 cells in the module would have 3 mΩ of series resistance and the same 2 cells would have 2.5 mΩ and 3.5 mΩ series resistance. In both cases, the module series resistance will be the same. This suggests that in some cases the SOH of individual cells cannot be reflected on module level. The implication of this is that EIS cannot be successfully compared between different modules. In order to do that, other additional information about the individual cells is needed.

V. CONCLUSION

An evaluation study has been performed on the consistency of EIS measurements performed at both cell and module levels. Following the EIS measurements on six individual cells, modules have been made by connecting the pre-characterized cells in series. Each time after adding a cell to the module, an

EIS measurement on the module consisting of 2 to 6 cells has been performed. The electrical components of the cell and module ECM were determined by curve fitting to the Nyquist plot from the EIS results. The combined result of the parameter values of the individual cells was compared to those of the whole module for 10%, 40% and 100% SOC. From the results, it appears that there is a clear correlation between the EIS results of the individual cells and of the module made by putting the cells in series. So our study concludes that EIS measurements can be performed at module level with an acceptable range of accuracy and good consistency with the results on the individual cells. The minor differences that were found can be attributed to stray capacitances, resistances of the cell interconnections, inaccuracy of the EIS equipment, and curve fitting inaccuracies. It is essential to mention the applicability of this method is a function of the homogeneity between the cells inside the module. For the modules and packs during the ageing there is a real need to expand the method by adding extra health factors beyond the EIS measurement on the module or pack.

Our future work will concern other cell chemistries and a further evaluation of the accuracy limitations of the experiment such as determination of stray resistances and capacitances. The method can furthermore be expanded by testing the individual cells for different health factors, for instance, parameters related to the voltage of each individual cell, which reflects the cell's health condition simultaneously while measuring the EIS on the whole module.

VI. Acknowledgement

We gratefully acknowledge the support and contribution of the late professor Braham Ferreira in the early stage of this research. Eduard Aguilar Boj is acknowledged for his support in the performing the experiments and for useful discussions on the results.

This work has been financially supported by the European Regional Development Fund (ERDF) as part of the Storage of Energy and Power Systems (STEPS) research project framework.

References

[1] European Commission, "Stepping up Europe's 2030 climate ambition Investing in a climate-neutral future for the benefit of our people," vol. 53, no. 9, pp. 1689–1699, 2020, ISSN: 1098-6596.

[2] M. Knipper, N. Ó Brolcháin, A. De Shryver, *et al.*, *State of the Art Report on Storage Technologies, Opportunities and Trends*, English, P. Mouratidis, Ed. Interreg North-West Europe, May 2021.

[3] B. Ferreira, "Batteries, the New Kids on the Block," *IEEE Power Electronics Magazine*, vol. 6, no. 4, pp. 32–34, Dec. 2019, ISSN: 23299215. DOI: 10.1109/MPEL.2019.2947980.

[4] S. Azizighalehsari, J. Popovic, P. Venugopal, and B. Ferreira, "A Review of Lithium-ion Batteries Diagnostics and Prognostics Challenges; A Review of Lithium-ion Batteries Diagnostics and Prognostics Challenges," *IECON 2021 - 47th Annual Conference of the IEEE Industrial Electronics Society*, 2021. DOI: 10.1109/IECON48115.2021.9589204.

[5] "Global EV Outlook 2021," IEA, Paris, France, Tech. Rep., 2021. [Online]. Available: https://www.iea.org/reports/global-ev-outlook-2021.

[6] M. H. S. M. Haram, J. W. Lee, G. Ramasamy, E. E. Ngu, S. P. Thiagarajah, and Y. H. Lee, "Feasibility of utilising second life EV batteries: Applications, lifespan, economics, environmental impact, assessment, and challenges," *Alexandria Engineering Journal*, vol. 60, no. 5, pp. 4517–4536, Oct. 2021, ISSN: 1110-0168. DOI: 10.1016/J.AEJ.2021.03.021.

[7] *This Dutch football stadium creates its own energy and stores it in electric car batteries — World Economic Forum*. [Online]. Available: https://www.weforum.org/agenda/2018/07/netherlands-football-johan-cruijff-stadium-electric-car-batteries/.

[8] M. Shahjalal, P. K. Roy, T. Shams, *et al.*, "A review on second-life of Li-ion batteries: prospects, challenges, and issues," *Energy*, vol. 241, 2022.

[9] S. Azizighalehsari, P. Venugopal, D. P. Singh, and G. Rietveld, "Performance Evaluation of Retired Lithium-ion Batteries for Echelon Utilization," *IECON 2022 - 48th Annual Conference of the IEEE Industrial Electronics Society (17-20 October)*, 2022.

[10] Q. Zhang, X. Li, Z. Du, and Q. Liao, "Aging performance characterization and state-of-health assessment of retired lithium-ion battery modules," *Journal of Energy Storage*, vol. 40, p. 102 743, Aug. 2021, ISSN: 2352-152X. DOI: 10.1016/J.EST.2021.102743.

[11] Z. Ning, Z. Deng, J. Li, H. Liu, and W. Guo, "Co-estimation of state of charge and state of health for 48 v battery system based on cubature kalman filter and h-infinity," *Journal of Energy Storage*, vol. 56, p. 106 052, 2022.

[12] A. Basia, Z. Simeu-Abazi, E. Gascard, and P. Zwolinski, "Review on state of health estimation methodologies for lithium-ion batteries in the context of circular economy," *CIRP Journal of Manufacturing Science and Technology*, vol. 32, pp. 517–528, 2021, ISSN: 1755-5817. DOI: https://doi.org/10.1016/j.cirpj.2021.02.004. [Online]. Available: https://www.sciencedirect.com/science/article/pii/S1755581721000249.

[13] K. M. Carthy, H. Gullapalli, K. M. Ryan, and T. Kennedy, "Electrochemical impedance correlation analysis for the estimation of Li-ion battery state of charge, state of health and internal temperature," *Journal of Energy Storage*, vol. 50, 2022.

[14] F. L. Daniel Kehl Torben Jennert and M. Kurrat, "Electrical characterization of li-ion battery modules for second-life applications," *MDPI*, vol. 32, 2021.

[15] H. Watanabea, S. Yoshina, H. I. Shitanda, and M. Itagaki, "Electrochemical impedance analysis on positive electrode in lithium-ion battery with galvanostatic control," *Journal of Power Sources*, vol. 507, 2021.

[16] N. Meddings, M. Heinrich, F. Overney, *et al.*, "Application of electrochemical impedance spectroscopy to commercial Li-ion cells: A review," *Journal of Power Sources*, vol. 480, no. July, 2020, ISSN: 03787753. DOI: 10.1016/j.jpowsour.2020.228742.

[17] U. Westerhoff, K. Kurbach, F. Lienesch, and M. Kurrat, "Analysis of lithium-ion battery models based on electrochemical impedance spectroscopy," *Energy Technology*, vol. 4, no. 12, pp. 1620–1630, 2016.

[18] P. Iurilli and C. Brivio and V. Wood, "On the use of electrochemical impedance spectroscopy to characterize and model the aging phenomena of lithium-ion batteries: a critical review," *Journal of Power Sources*, vol. 505, 2021.

[19] P. Iurilli, C. Brivio, and V. Wood, "On the use of electrochemical impedance spectroscopy to characterize and model the aging phenomena of lithium-ion batteries: a critical review," *Journal of Power Sources*, vol. 505, p. 229 860, Sep. 2021, ISSN: 0378-7753. DOI: 10.1016/J.JPOWSOUR.2021.229860.